Template Synthesis, Crystal Structure and Luminescent Properties of Neutral N_4O_3 Tripodal $Ln^{III}L$ Complexes (Ln^{III} = La^{3+}, Eu^{3+}, Gd^{3+}, Tb^{3+}, Dy^{3+}, Ho^{3+}, Er^{3+}, Tm^{3+} or Lu^{3+}; H_3L = Tris{[3′-(2′′-pyridyl)-5′-*tert*-butyl-2′-hydroxybenzylidene-2-imino]ethyl}amine)

Wai-Kwok Wong,*[a] Hongze Liang,[a] Jianping Guo,[a] Wai-Yeung Wong,[a] Wing-Kit Lo,[a] King-Fai Li,[b] Kok-Wai Cheah,[b] Zhongyuan Zhou,[c] and Wing-Tak Wong[d]

Keywords: Lanthanides / Luminescence / Schiff bases / Tripodal ligands

In the presence of Ln^{3+} (Ln = La, Eu, Gd, Tb, Dy, Ho, Er, Tm or Lu), tris(2-aminoethyl)amine condensed with three equivalents of 3-(2′-pyridyl)-5-*tert*-butyl-2-hydroxybenzaldehyde in methanol to give the neutral Schiff-base complex $Ln^{III}L$ (Ln = La **1**, Eu **2**, Gd **3**, Tb **4**, Dy **5**, Ho **6**, Er **7**, Tm **8** and Lu **9**; H_3L = tris{[3′-(2′′-pyridyl)-5′-*tert*-butyl-2′-hydroxybenzylidene-2-imino]ethyl}amine). The structures of compounds **4**–**7** were determined by X-ray crystallography. The crystal structure analyses revealed that the Schiff base behaves as a tri-deprotonated heptadentate ligand encapsulating the lanthanide metal ion within the N_4O_3 cavity, with all the pyridyl groups being pendant. Solution spectroscopic data suggest that the $Ln^{III}L$ complexes remain intact in methanol and exist as nine-coordinate non-electrolytes with the lanthanide metal ions coordinated to the N_4O_3 cavity of the tripodal Schiff base and two solvent molecules. The solution photoluminescent properties of these lanthanide Schiff-base complexes were also examined.
(© Wiley-VCH Verlag GmbH & Co. KGaA, 69451 Weinheim, Germany, 2004)

Introduction

The potential application of lanthanide complexes as magnetic resonance contrasting agents has led to the synthesis of a number of lanthanide(III) complexes with heptadentate tripodal Schiff-base ligands and amine phenol ligands.[1−4] Numerous lanthanide complexes with macrocyclic polydentate Schiff-base ligands[5−8] and acyclic tripodal heptadentate Schiff-base ligands have been reported in the literature.[1,2,9−12] Recently, the coordination chemistry of the decadentate Schiff base tris[4-(2-hydroxy-3-methoxyphenyl)-3-aza-3-butenyl]amine toward p- and f-block elements[13−17] has been examined. Dinuclear homo-[13] and heterometallic[14−17] complexes were obtained. Some lanthanide ions possess strongly emissive and long-lived excited states, such as Eu^{3+} and Tb^{3+}, but do not exhibit intense absorption bands. Therefore, considerable effort has been devoted to the design of lanthanide complexes where light is absorbed by the ligands and the corresponding electronic energy is then transferred onto the emitting metal ion. The use of a Zn^{2+} Schiff-base complex as a sensitizer for Nd^{3+}, Yb^{3+} and Er^{3+} near-infrared luminescence has been reported recently.[18] We are interested in the coordination chemistry of the decadentate Schiff base tris{[5′-*tert*-butyl-2′-hydroxy-3′-(2′′-pyridyl)benzylidene-2-imino]-ethyl}amine (H_3L) toward f-block metal ions, and particularly its sensitizing effect on lanthanide(III) metal ions. The design of the ligand strands of H_3L prevents the introduction of metal ions into the terminal nine-coordinate cavity, as this would result in the formation of fused chelating six-membered rings. Thus, H_3L is expected to behave as a heptadentate podate with the inner N_4O_3 cavity coordinating to the lanthanide ions and the terminal 2-pyridyl groups pendant, and will be an ideal ligand used for the preparation of heterometallic complexes. In this report, we describe a one-pot synthesis and the photoluminescent properties of stable, neutral, polydentate Schiff-base complexes of lanthanide(III) metal ions.

[a] Department of Chemistry, Hong Kong Baptist University
Waterloo Road, Kowloon Tong, Hong Kong, P. R. China
Fax: (internat.) + 852-3411-5862
E-mail: wkwong@hkbu.edu.hk
[b] Department of Physics, Hong Kong Baptist University
Waterloo Road, Kowloon Tong, Hong Kong, P. R. China
[c] Department of Applied Biology and Chemical Technology, Hong Kong Polytechnic University
Hung Hom, Hong Kong, P. R. China
[d] Department of Chemistry, The University of Hong Kong
Pokfulam Road, Hong Kong, P. R. China

Results and Discussion

Synthesis and Characterization

In the presence of one equivalent of $Ln(NO_3)_3{\cdot}5H_2O$ (Ln = La, Eu, Gd, Tb, Dy, Ho, Er, Tm or Lu), tris(2-

aminoethyl)amine (tren) undergoes condensation with three equivalents of 5-*tert*-butyl-2-hydroxy-3-(2′-pyridyl)benzaldehyde (Py-CHO) in methanol to give the neutral tripodal Schiff-base complexes $Ln^{III}L$ (Ln = La **1**, Eu **2**, Gd **3**, Tb **4**, Dy **5**, Ho **6**, Er **7**, Tm **8** and Lu **9**; H_3L = tris{[5′-*tert*-butyl-2′-hydroxy-3′-(2′′-pyridyl)benzylidene-2-imino]-ethyl}amine) in moderate to good yields (Scheme 1). Compounds **1**−**9** are remarkably stable towards air and moisture, are soluble in many organic solvents, and are even stable in protic solvents for weeks. They also show high thermal stability: when heated to as high as 200 °C, no discernible collapse of the crystals was observed. All these compounds gave satisfactory elemental analyses and exhibit a $\nu_{C=N}$ band at 1621−1623 cm^{-1} in their IR spectra and an $[M + H]^+$ peak in their positive FAB mass spectra. The structures of compounds **4**−**7** were determined by X-ray crystallography.

Compounds **4**−**7** are isomorphous and they all crystallized in the triclinic space group $P\bar{1}$ with two independent, but structurally similar, molecules per asymmetric unit. The crystal structure analyses reveal that the potentially decadentate tripodal ligand acts as a heptadentate ligand with the Ln^{3+} ion encapsulated within the N_4O_3 cavity of the Schiff base; all the pyridyl groups remain uncoordinated. A perspective drawing of **4** is shown in Figure 1.

For **4**, the Tb^{3+} ion is seven coordinate and its geometry can be considered as a mono-capped octahedron with the tertiary amine nitrogen N(4) capped on the triangular face formed by the three imino nitrogen atoms. The Tb−N distance of the capped tertiary nitrogen [Tb(1)−N(4) 2.686(4) Å] is longer than those of the imino nitrogens [Tb(1)−N(1) 2.456(4), Tb(1)−N(2) 2.475(4) and Tb(1)−N(3) 2.486(4) Å]. The Tb−O distances are 2.187(3) [Tb(1)−O(1)], 2.216(3) [Tb(1)−O(2)] and 2.205(3) Å [Tb(1)−O(3)]. The Tb−N(amino) distance and average Tb−N(imino) distance (2.472 Å) are slightly shorter than, whereas the average Tb−O (2.203 Å) distance is similar to, those of Pr(trensal)[9] [Pr−N(amino) 2.805(5), Pr−N(imino) 2.620 and Pr−O 2.282 Å] and Nd(trensal)[9] [Nd−N(amino) 2.799(4), Nd−N(imino) 2.601 and Nd−O 2.275 Å], after considering the influence of the lanthanide contraction. The carbon−nitrogen distances for the imino nitrogens [N(1)−C(1) 1.279(6), N(2)−C(32) 1.264(7) and N(3)−C(39) 1.258(8) Å] are in agreement with the C=N distance. All the pyridyl groups are pointing away from the metal and are not coplanar with the phenyl rings of the Schiff-base ligand. The torsion angles between the phenyl rings and the pyridyl groups are −33.4° [C(16)−C(10)−C(11)−C(15)], 37.7° [C(17)−C(18)−C(19)−C(23)] and 27.7° [C(54)−C(48)−C(49)−C(53)]. The

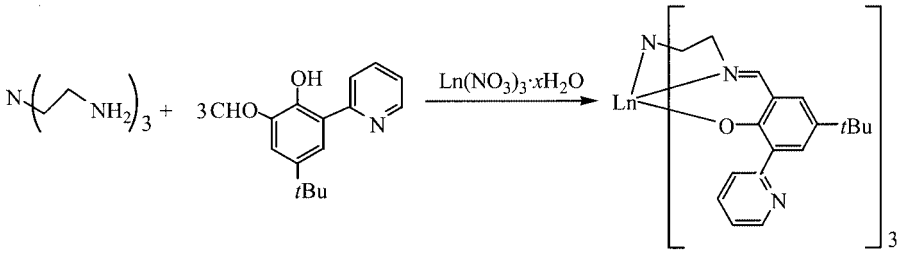

Ln = La **1**, Eu **2**, Gd **3**, Tb **4**, Dy **5**, Ho **6**, Er **7**, Tm **8**, Lu **9**

Scheme 1

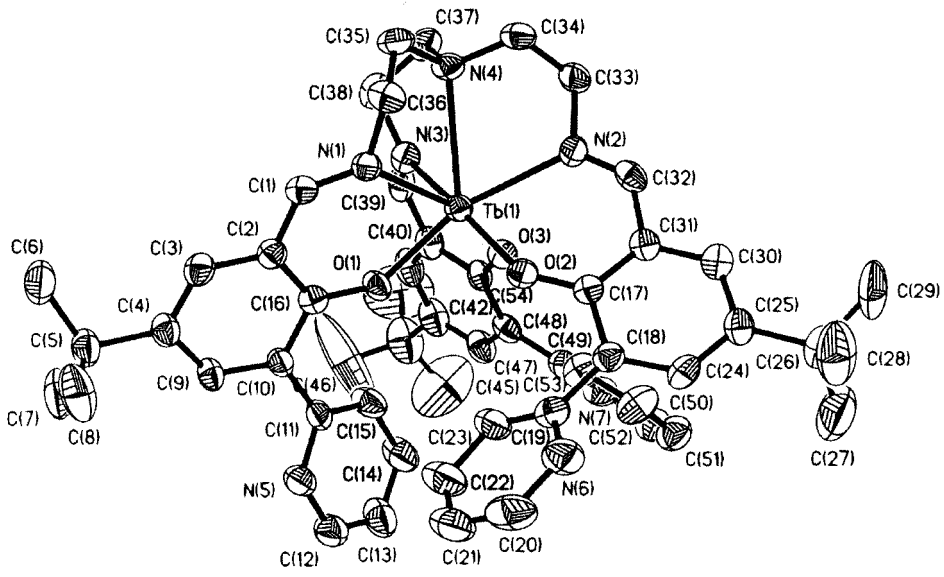

Figure 1. A perspective drawing of one molecule of compound **4**; hydrogen atoms are omitted for clarity

 © 2004 Wiley-VCH Verlag GmbH & Co. KGaA, Weinheim

Table 1. Selected bond lengths (Å) and bond angles (°) for compounds **4**−**7**

	4 (M = Tb)	**5** (M = Dy)	**6** (M = Ho)	**7** (M = Er)
M(1)−O(1)	2.187(3)	2.197(7)	2.1856(16)	2.180(5)
M(1)−O(2)	2.216(3)	2.198(7)	2.1858(18)	2.172(5)
M(1)−O(3)	2.205(3)	2.210(8)	2.1948(18)	2.189(5)
M(1)−N(1)	2.456(4)	2.437(8)	2.432(2)	2.662(6)
M(1)−N(2)	2.475(4)	2.476(10)	2.457(2)	2.455(6)
M(1)−N(3)	2.486(4)	2.474(9)	2.480(2)	2.410(6)
M(1)−N(4)	2.686(4)	2.685(8)	2.678(2)	2.468(7)
N(1)−C(imine)	1.279(6)	1.284(12)	1.285(3)	1.250(10)
N(2)−C(imine)	1.264(7)	1.289(14)	1.273(4)	1.292(8)
N(3)−C(imine)	1.258(8)	1.253(13)	1.274(3)	1.266(10)
O(1)−M(1)−O(2)	89.05(13)	90.8(3)	89.54(6)	88.8(2)
O(1)−M(1)−O(3)	90.70(12)	88.6(3)	88.97(7)	93.8(2)
O(2)−M(1)−O(3)	92.77(13)	93.7(3)	92.76(7)	89.8(2)
N(1)−M(1)−N(2)	114.86(14)	97.4(3)	95.98(7)	68.2(2)
N(1)−M(1)−N(3)	95.50(14)	114.0(3)	114.33(7)	67.5(2)
N(1)−M(1)−N(4)	66.50(12)	68.0(3)	66.88(6)	67.3(2)
N(2)−M(1)−N(3)	106.83(14)	107.4(3)	107.49(7)	112.3(2)
N(2)−M(1)−N(4)	68.17(13)	67.0(3)	67.54(8)	107.8(2)
N(3)−M(1)−N(4)	66.88(14)	67.9(3)	67.72(7)	99.2(2)
O(1)−M(1)−N(1)	72.58(13)	72.8(3)	73.58(6)	123.5(2)
O(1)−M(1)−N(2)	160.55(13)	89.6(3)	88.26(7)	73.3(2)
O(1)−M(1)−N(3)	89.63(14)	160.0(3)	160.81(7)	92.0(2)
O(1)−M(1)−N(4)	129.51(12)	130.3(3)	130.10(6)	167.2(2)

structures of compounds **5**−**7** are very similar to that of **4** and will not be discussed in detail here. Selected bond lengths and bond angles for compounds **4**−**7** are collectively listed in Table 1. Important structural properties of compounds **4**−**7** are given in Table 2. The M−N(imino), M−N(amino) and M−O(phenoxy) bond lengths decrease from **4** to **7**, reflecting the general rule of lanthanide contraction from the early to late f-elements.

Table 2. Structural properties of compounds **4**−**7**

	4	**5**	**6**	**7**
M−N(amino) (Å)	2.686	2.685	2.678	2.662
Average M−N(imino) (Å)	2.472	2.462	2.456	2.444
Average M−O (Å)	2.203	2.202	2.189	2.180
Torsion angle (°) [a]	**I** −33.4	**I** −33.0	**I** −34.8	**I** −35
	II 27.7	**II** 27.2	**II** 26.3	**II** 28
	III 37.7	**III** 36.0	**III** 36.8	**III** 35

[a] Torsion angles: **4** [**I** C(16)−C(10)−C(11)−C(15), **II** C(54)−C(48)−C(49)−C(53), **III** C(17)−C(18)−C(19)−C(23)]; **5** [**I** C(4)−C(5)−C(6)−C(7), **II** C(22)−C(23)−C(24)−C(25), **III** C(40)−C(41)−C(42)−C(43)]; **6** [**I** C(1)−C(2)−C(3)−C(4), **II** C(31)−C(30)−C(32)−C(33), **III** C(49)−C(48)−C(50)−C(51)]; **7** [**I** C(27)−C(26)−C(32)−C(33), **II** C(45)−C(44)−C(50)−C(51), **III** C(9)−C(8)−C(14)−C(15)].

Conductivity measurements show that compounds **1**−**9** behave as non-electrolytes in methanol solution. The electrospray ionization high-resolution mass spectrum (positive mode) of each complex in methanol shows a mass peak at *m*/*z* corresponding to $[M + H]^+$. For instance, the Eu^{3+} complex exhibits the mass peak at *m*/*z* = 1008.4032, which deviates less than 5 ppm from the theoretical peak value of 1008.4048 for the elemental composition $C_{54}H_{61}EuN_7O_3$. The observed isotopic distribution patterns of the $[M + H]^+$ peaks match well with the expected theoretical signals. The ^1H NMR spectrum of the Lu complex **9** in CD_3OD displays a single set of resonances attributed to the *tert*-butyl protons at δ = 1.35 (s, 27 H), the NCH_2CH_2N protons at δ = 2.82 (t, $J_{H,H}$ = 6.5 Hz, 6 H) and 3.10 ppm (t, $J_{H,H}$ = 6.5 Hz, 6 H), the 2-pyridyl protons at δ = 7.02 (t, $J_{H,H}$ = 6.5 Hz, 3 H), 7.15 (m, 3 H), 7.53 (m, 3 H) and 8.11 ppm (d, $J_{H,H}$ = 8.1 Hz, 3 H), the phenyl protons at δ = 7.63 (s, 3 H) and 8.00 ppm (s, 3 H) and the -N=C*H*- protons at δ = 8.47 ppm (s, 3 H). This indicates that there is only one species present in solution and the solution structure of the complex is similar to its solid-state structure, with the lanthanide ion coordinated in the N_4O_3 cavity of the ligand with pendant 2-pyridyl groups rotating freely in solution. Furthermore, luminescent studies (vide infra) on Eu^{3+} and Tb^{3+} complexes indicate that there are two methanol molecules coordinated to the lanthanide ions. The above data suggest that compounds **1**−**9** exist as nine-coordinate non-electrolytes in methanol solution, with the lanthanide metal ions coordinated in the N_4O_3 cavity of the tripodal ligand and also to two solvent molecules.

Photophysical Properties

At room temperature, compounds **1**−**9** exhibit similar solution absorption and emission spectra in the UV/Vis region. Their photophysical properties are summarized in Table 3. The absorptions between 255 and 383 nm can be assigned to $\pi \rightarrow \pi^*$ transitions of the tripodal Schiff-base ligand. The visible emission of compounds **1**−**9**, with lifetimes (τ) ranging from 3.8 to 9.4 ns and quantum yields (Φ_{em}) of 0.33−5.57 × 10^{-2}, can be assigned to the intra-

 © 2004 Wiley-VCH Verlag GmbH & Co. KGaA, Weinheim

Table 3. Photophysical data of compounds **1**−**9**[a]

Compound	Absorption λ_{max}/nm [log(ε/dm^3 mol^{-1} cm^{-1})]	Excitation λ_{exc}/nm	Emission λ_{em}/nm (τ/ns, $\Phi_{em} \times 10^2$)[b]
1	381 (3.99), 255 (4.39)	380	460 (9.4, 1.36)
2	380 (4.33), 255 (4.75)	380	470 (4.5, 0.46)
3	384 (4.09), 258 (4.53)	380	455 (3.8, 0.21)[c]
4	382 (4.30), 256 (4.68)	380	466 (4.7, 2.38)
5	382 (4.42), 257 (4.80)	380	466 (4.7, 1.27)
6	381 (4.29), 256 (4.70)	380	469 (4.6, 5.57)
7	383 (4.52), 256 (4.89)	380	466 (4.7, 2.29)
8	382 (4.33), 256 (4.71)	380	453 (4.5, 0.33)
9	378 (3.97), 256 (4.35)	380	460 (4.5, 3.62)[d]

[a] Photophysical measurements were made in $2 \cdot 10^{-5}$ M CH_3OH solution at room temperature. [b] Quantum yields were determined relative to quinine sulfate in 0.1 N H_2SO_4 ($\Phi = 0.55$). [c] Phosphorescence band was also observed at 508 nm ($\tau = 776$ μs). [d] Phosphorescence band was also observed at 500 nm ($\tau = 26.3$ ms).

ligand emission. The absorption, emission and excitation (monitored at 465 nm) spectra of **7** are shown in Figure 2. The photoluminescence excitation (PLE) spectrum reflects where the maximum contribution of the photoluminescence (PL) comes from. Under steady-state conditions, excited electrons relax from the highest excited states to the lowest excited states before they recombine radiatively or non-radiatively. In this case, the PLE spectrum shows exactly this situation; the maximum PL contribution comes from the lowest excited bands, with a decreasing contribution from the higher-energy band. Thus, although the absorption bands coincide with the excitation bands, as they should, the relative intensities of the energy bands by the two techniques can reveal the origin of the physical process measured. The emission spectra and decay time measurements for Gd^{3+} complexes allowed the identification of the lowest ligand triplet state in the complexes.[19−22] This is possible because the metal-centered (MC) electronic levels of Gd^{3+} are known to be located at 31000 cm^{-1}, typically well above the ligand-centered electronic levels of aromatic ligands.[23] Therefore, ligand-to-metal energy transfer and the consequent MC luminescence cannot be observed.

Figure 3 shows the variable temperature emission spectra of **3** in methanol. The time-resolved spectra of **3** show that at room temperature the lifetimes at 455 and 508 nm are

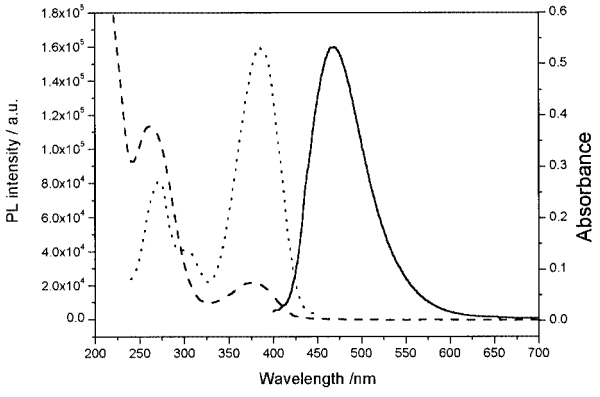

Figure 2. Room temperature absorption (− − − −), emission (———; excited at 380 nm) and excitation (·····; monitored at 465 nm) spectra of **7** in CH_3OH

both 3.8 ns, indicating that the emissions come from the same state and correspond to a ligand-centered (LC) short-lived fluorescence. At 77 K, on top of the weak LC fluorescence ($\tau = 4.1$ ns at 455 nm and 6.8 ns at 508 nm), an intense LC long-lived phosphorescence is also observed at 508 nm ($\tau = 776$ μs). This indicates that both LC singlet and triplet states exist at 77 K. The ligand-centered excited singlet state (^{1}LC) is estimated to be about 22000 cm^{-1} and the triplet state (^{3}LC) to be 19690 cm^{-1}.

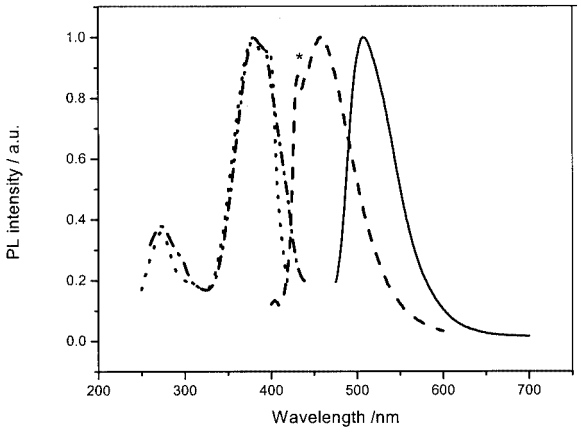

Figure 3. Variable-temperature emission and excitation spectra of **3** in CH_3OH; room temperature emission (− − −; excited at 380 nm) and excitation (·····; monitored at 455 nm) spectra, 77 K emission (———; excited at 380 nm) and excitation (−·−·−; monitored at 508 nm) spectra; the peak marked with an asterisk is due to scattering

The variable-temperature photoluminescent properties of compounds **2**, **4** and **7** in methanol have also been examined. Emission corresponding to the characteristic 4f−4f transitions of trivalent lanthanide metal ions was observed at 77 K but not at room temperature for **2** and **4**. Figure 4 and 5 show the room temperature and 77 K emission and excitation spectra of **2** and **4**, respectively. At room temperature, the time-resolved spectra of **2** and **4** taken at their emission peak ($\lambda_{max} = 470$ nm for **2**, $\tau = 4.5$ ns; $\lambda_{max} = 466$ nm for **4**, $\tau = 4.7$ ns) and 508 nm ($\tau = 4.5$ ns for **2** and 4.7 ns for **4**) show that the emission corresponds to a li-

 © 2004 Wiley-VCH Verlag GmbH & Co. KGaA, Weinheim

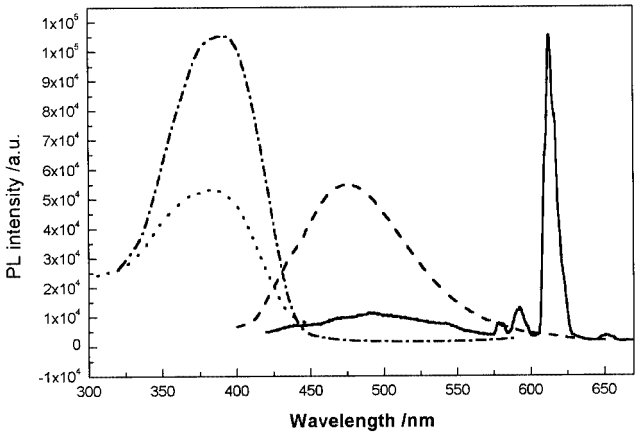

Figure 4. Variable-temperature emission and excitation spectra of **2** in CH_3OH; room temperature emission (– – –; excited at 380 nm) and excitation (·····; monitored at 465 nm) spectra, 77 K emission (———; excited at 380 nm) and excitation (–·–·–; monitored at 613 nm) spectra

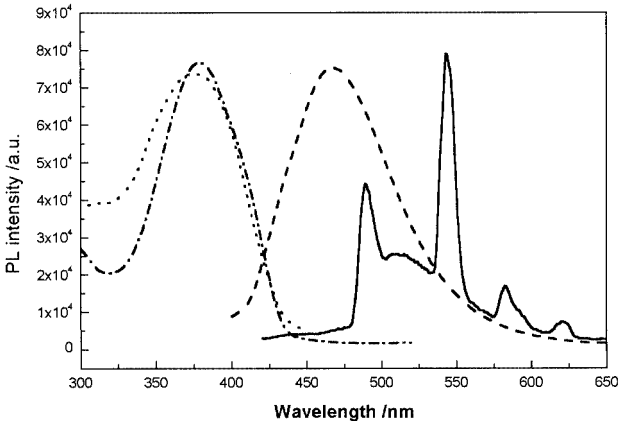

Figure 5. Variable-temperature emission and excitation spectra of **4** in CH_3OH; room temperature emission (– – –; excited at 380 nm) and excitation (·····; monitored at 465 nm) spectra, 77 K emission (———; excited at 380 nm) and excitation (–·–·–; monitored at 544 nm) spectra

gand-centered (^{1}LC) short-lived fluorescence. At 77 K, the lanthanide ion emission for compound **2**, which has a lifetime of 476 μs in CH_3OH and 787 μs in CD_3OD, corresponds to the $^5D_0 \rightarrow {}^7F_J$ transitions of Eu^{3+}, with the emission at 611 nm being assigned to the $^5D_0 \rightarrow {}^7F_2$ transition.[24] Other than the Eu^{3+} emission, a very broad and weak emission peak at around 470 nm was also observed at 77 K (Figure 4). Lifetime measurements confirmed that the emission was purely ^{1}LC fluorescence with no ^{3}LC phosphorescence (τ being 4.9 ns at 470 nm and 5.4 ns at 508 nm). The observation of ^{3}LC phosphorescence for the Gd^{3+} complex (**3**) but not for the Eu^{3+} complex (**2**) indicates that energy transfer from the ligand triplet ^{3}LC to Eu^{3+} excited states is quite efficient. The emission for compound **4** at 77 K, which has a lifetime of 572 μs in CH_3OH and 678 μs in CD_3OD, corresponds to the $^5D_4 \rightarrow {}^7F_J$ transitions of Tb^{3+}, with the emission centered at 551 nm arising from the $^5D_4 \rightarrow {}^7F_5$ transition.[24] Other than the Tb^{3+} emission, a very broad and weak emission centered around 466 nm and a medium-strong emission centered around 508 nm were also observed at 77 K (Figure 5). The time-resolved spectra show that there is only one lifetime at 466 nm (τ being 5.6 ns) and two different lifetimes at 508 nm (τ being 6.0 ns and 113 μs). This shows that the emission centered at 466 nm is due to ^{1}LC fluorescence and that at 508 nm to ^{3}LC phosphorescence. Unlike **2**, which does not show any ^{3}LC phosphorescence, **4** exhibits ^{3}LC phosphorescence, which is probably due to back energy-transfer from the metal excited state to the ^{3}LC. It has been shown that efficient back energy-transfer takes place in Tb^{3+} complexes when ΔE (^{3}LC – $^5D_4$) is less than 1850 cm^{-1}.[25] The energy of the ligand triplet state is about 2400 cm^{-1} higher than the energy of the $^5D_0$ Eu^{3+} luminescent level (17300 cm^{-1}) and lies at almost the same energy as the $^5D_4$ Tb^{3+} luminescent level (20450 cm^{-1}).[23] Thus, efficient ligand-to-metal energy transfer is observed for the Eu^{3+} complex and significant back energy-transfer for the Tb^{3+} complex. The excitation band of **2** (monitored at 613 nm for Eu^{3+}) and **4** (monitored at 545 nm for Tb^{3+}) is located around 380 nm in each case, and closely resembles their low-energy absorption band, indicative of their similar ori-

Table 4. Photophysical data of compounds **2** and **4** at 77 K[a]

Compound	Excitation (nm)	Emission (nm)	Transition	τ in CH_3OH[b] (μs)	τ in CD_3OD[b] (μs)
2	382	579	$^5D_0 \rightarrow {}^7F_0$		
		593	$^5D_0 \rightarrow {}^7F_1$		
		613	$^5D_0 \rightarrow {}^7F_2$		
		651	$^5D_0 \rightarrow {}^7F_3$	476	787
		681	$^5D_0 \rightarrow {}^7F_4$		
4	380	489	$^5D_4 \rightarrow {}^7F_6$		
		543	$^5D_4 \rightarrow {}^7F_5$	572	678
		582	$^5D_4 \rightarrow {}^7F_4$		
		621	$^5D_4 \rightarrow {}^7F_3$		

[a] Photophysical measurements were made in a $2 \cdot 10^{-5}$ M CH_3OH or CD_3OD solution at 77 K. [b] Measured in correspondence with the most intense emission band ($^5D_0 \rightarrow {}^7F_2$ for Eu^{3+} and $^5D_4 \rightarrow {}^7F_5$ for Tb^{3+}).

 © 2004 Wiley-VCH Verlag GmbH & Co. KGaA, Weinheim

gin. This clearly shows that the excitation of both Eu^{3+} and Tb^{3+} complexes originates from the $\pi \rightarrow \pi^*$ transitions of the Schiff-base antenna. Their low-temperature photophysical properties and assignments of the transitions are summarized in Table 4. Based on the different lifetimes of the lanthanide-ion emissions in CH_3OH and CD_3OD, the number of coordinated methanol molecules (*n*), which can be calculated from Horrocks equation,[26] is estimated to be 1.74 and 2.30 for Eu^{3+} and Tb^{3+}, respectively. This indicates that in methanol solution, there are two solvent molecules coordinated to the trivalent lanthanide metal ions.

However, even at 77 K, **7** exhibits no ^{3}LC emission in the visible region nor an emission corresponding to the $^4I_{13/2} \rightarrow {}^4I_{15/2}$ transition of Er^{3+} in the near-infrared region. This suggests that the Er^{3+} ion probably relaxes its energy, which it receives from the antenna, via vibrational modes to the environment.

Conclusion

In this paper, we have demonstrated that lanthanide Schiff-base complexes, $Ln^{III}L$, can be conveniently prepared by the condensation of tris(2-aminoethyl)amine with three equivalents of 5-*tert*-butyl-2-hydroxy-3-(2′-pyridyl)benzaldehyde in the presence of trivalent lanthanide metal ions. A photophysical study shows that the Schiff-base ligand can act as an antenna and transfer the absorbed light energy via its triplet state to the Eu^{3+} and Tb^{3+} metal ions.

Experimental Section

General Procedures: All reactions were carried out under an atmosphere of dry nitrogen. Solvents were dried by standard procedures, and distilled and deaerated prior to use. Hydrated lanthanide salts and tris(2-aminoethyl)amine (tren) were obtained from the Aldrich Chemical Company and used without further purification. 5-*tert*-Butyl-2-hydroxy3-(2′-pyridyl)benzaldehyde (Py-CHO) was prepared according to a literature method.[27] Microanalyses were performed by the Shanghai Institute of Organic Chemistry, Chinese Academy of Sciences, China. Electronic absorption spectra in the UV/Vis region were recorded on a Hewlett−Packard 8453 UV/Visible spectrophotometer, steady-state visible fluorescence and PL excitation spectra on a Photon Technology International (PTI) Alphascan spectrofluorimeter and visible decay spectra on a pico-N_2 laser system (PTI Time Master) with λ_{exc} = 337 nm. Quantum yields were computed according to a literature method[28] using quinine sulfate in 0.1 N H_2SO_4 as the reference standard (Φ = 0.55 in air-equilibrated water).[29] The number of coordinated solvent molecules (*n*) for the Eu^{3+} and Tb^{3+} complexes was calculated from the Horrocks equation $n = r(\tau_H^{-1} - \tau_D^{-1})$, where τ_H and τ_D are the excited-state lifetimes (in ms) in CH_3OH and CD_3OD, respectively, and the value of *r* is 2.1 and 8.4 for Eu^{3+} and Tb^{3+}, respectively.[26] Infrared spectra (KBr pellets) were recorded on a Nicolet Nagna-IR 550 spectrometer and NMR spectra on a JEOL EX270 spectrometer. Chemical shifts of ^{1}H NMR spectra were referenced to internal deuterated solvents and then recalculated to $SiMe_4$ (δ = 0.00 ppm). Low-resolution mass spectra (LRMS) were obtained on a Finnigan MAT SSQ-710 spectrometer in the positive FAB mode. Electrospray ionization high-resolution mass spectra (ESI-HRMS) were recorded on a QSTAR mass spectrometer. Conductivity measurements were carried out with a DDS-11 conductivity bridge for 10^{-4} mol dm^{-1} solutions in methanol.

Preparation of Lanthanide Schiff-Base Complexes: Compounds **1**−**9** were prepared using a similar method. A typical procedure for the preparation of the complexes is given for **1**.

Compound 1: A solution of $La(NO_3)_3{\cdot}6H_2O$ (0.044 g, 0.102 mmol) and Py-CHO (0.077 g, 0.304 mmol) in methanol (15 mL) was heated to 55 °C. Then, a solution of tren (0.015 g, 0.103 mmol) in methanol (10 mL) was added and the mixture was refluxed for an additional 2 h. The solution was then cooled to room temperature, filtered and the solvents evaporated to dryness in vacuo. The residue was re-dissolved in dichloromethane, filtered and slowly evaporated in air to give yellow crystals, which were filtered and dried in vacuo. Yield: 0.078 g, 74%; m.p. > 260 °C (decomp). ^{1}H NMR (in CD_3OD): δ = 1.36 (s, 27 H, *tert*-butyl), 2.82 and 3.10 (2 × t, $J_{H,H}$ = 6.5 Hz, 2 × 6 H, 3 × NCH_2CH_2N), 7.24 (t, $J_{H,H}$ = 6.2 Hz, 3 H, py-H), 7.55 (s, 3 H, Ar-H), 7.60 (m, 3 H, py-H), 7.86 (s, 3 H, Ar-H), 8.19 (m, 3 H, py-H), 8.28 (d, $J_{H,H}$ = 9.4 Hz, 3 H, py-H), 8.34 (s, 3 H, N=C*H*) ppm. IR (KBr): $\nu_{C=N}$ = 1623 cm^{-1}. ESI-HRMS (+ve mode, CH_3OH): *m*/*z* = 994.3854 [M + H]$^+$ ($C_{54}H_{61}LaN_7O_3$ requires 994.3899). $C_{54}H_{60}LaN_7O_3{\cdot}3.5H_2O$ (1057.06): calcd. C 61.35, H 6.40, N 9.28; found C 61.45, H 6.34, N 9.32.

Compound 2: $Eu(NO_3)_3{\cdot}6H_2O$ (0.045 g, 0.101 mmol), Py-CHO (0.077 g, 0.304 mmol) and tren (0.015 g, 0.103 mmol) were used. Yield: 0.064 g, 60%; light-yellow solid, m.p. > 210 °C (decomp). IR (KBr): $\nu_{C=N}$ = 1621 cm^{-1}. MS (FAB, +ve): *m*/*z* = 1008 [M + H]$^+$ for ^{153}Eu. ESI-HRMS (+ve mode, CH_3OH): *m*/*z* = 1008.4032 [M + H]$^+$ ($C_{54}H_{61}EuN_7O_3$ requires 1008.4048). $C_{54}H_{60}EuN_7O_3{\cdot}3.5H_2O$ (1070.12): calcd. C 60.60, H 6.26, N 9.16; found C 60.40, H 6.26, N 9.39.

Compound 3: $Gd(NO_3)_3{\cdot}6H_2O$ (0.045 g, 0.100 mmol), Py-CHO (0.077 g, 0.304 mmol) and tren (0.015 g, 0.103 mmol) were used. Yield: 0.072 g, 68%; light-yellow solid, m.p. > 250 °C (decomp). IR (KBr): $\nu_{C=N}$ = 1628 cm^{-1}. ESI-HRMS (+ve mode, CH_3OH): *m*/*z* = 1013.4004 [M + H]$^+$ ($C_{54}H_{61}GdN_7O_3$ requires 1013.4077). $C_{54}H_{60}GdN_7O_3{\cdot}2.5H_2O$ (1057.39): calcd. C 61.32, H 6.21, N 9.27; found C 61.36, H 6.10, N 9.29.

Compound 4: $Tb(NO_3)_3{\cdot}6H_2O$ (0.045 g, 0.099 mmol), Py-CHO (0.077 g, 0.304 mmol) and tren (0.015 g, 0.103 mmol) were used. Yield: 0.073 g, 69%, greenish-yellow solid, m.p. > 200 °C (decomp). IR (KBr): $\nu_{C=N}$ = 1623 cm^{-1}. MS (FAB, +ve): *m*/*z* = 1014 [M + H]$^+$ for ^{159}Tb. ESI-HRMS (+ve mode, CH_3OH): *m*/*z* = 1014.4061 [M + H]$^+$ ($C_{54}H_{61}N_7O_3Tb$ requires 1014.4089). $C_{54}H_{60}N_7O_3Tb{\cdot}2.5H_2O$ (1059.06): calcd. C 61.23, H 6.20, N 9.26; found C 61.24, H 6.06, N 9.28.

Compound 5: $DyCl_3$ (0.027 g, 0.100 mmol), Py-CHO (0.077 g, 0.304 mmol) and tren (0.015 g, 0.103 mmol) were used. Yield: 0.074 g, 71%, greenish-yellow solid, m.p. > 250 °C (decomp). IR (KBr): $\nu_{C=N}$ = 1622 cm^{-1}. MS (FAB, +ve): *m*/*z* = 1019 [M + H]$^+$ for ^{164}Dy. ESI-HRMS (+ve mode, CH_3OH): *m*/*z* = 1019.4180 [M + H]$^+$ ($C_{54}H_{61}DyN_7O_3$ requires 1019.4127). $C_{54}H_{60}DyN_7O_3{\cdot}H_2O$ (1035.61): calcd. C 62.62, H 6.05, N 9.47; found C 62.43, H 6.04, N 9.37.

Compound 6: $Ho(NO_3)_3{\cdot}5H_2O$ (0.044 g, 0.100 mmol), Py-CHO (0.077 g, 0.304 mmol) and tren (0.015 g, 0.103 mmol) were used. Yield: 0.071 g, 63%, yellow solid, m.p. > 170 °C (decomp). IR

 © 2004 Wiley-VCH Verlag GmbH & Co. KGaA, Weinheim

Table 5. Crystallographic data for compounds **4**−**7**

Compound	**4**·H_2O	**5**·CH_3OH·0.75H_2O	**6**·1.5H_2O	**7**·2CH_3OH
Empirical formula	$C_{54}H_{60}N_7O_3Tb·H_2O$	$C_{54}H_{60}N_7O_3Dy·CH_3OH·0.75H_2O$	$C_{54}H_{60}N_7O_3Ho·1.5H_2O$	$C_{54}H_{60}N_7O_3Er·2CH_3OH$
Molecular mass	1032.03	1063.15	1047.05	1086.46
Crystal size [mm]	0.36 × 0.25 × 0.18	0.10 × 0.10 × 0.05	0.20 × 0.10 × 0.10	0.22 × 0.18 × 0.17
Crystal system	triclinic	triclinic	triclinic	triclinic
Space group	$P\bar{1}$	$P\bar{1}$	$P\bar{1}$	$P\bar{1}$
a [Å]	15.700(3)	15.965(4)	15.6849(13)	15.967(1)
b [Å]	18.443(4)	18.320(5)	18.4880(14)	18.439(1)
c [Å]	19.035(4)	19.257(5)	19.0286(15)	19.456(1)
α [°]	81.692(4)	79.563(6)	81.6340(10)	80.24(1)
β [°]	85.099(4)	83.795(7)	85.1270(10)	84.300(9)
γ [°]	75.021(4)	74.440(6)	75.0850(10)	74.13(1)
V [Å^3]	5262(2)	5326(3)	5268.8(7)	5421.6(8)
Z	4	4	4	4
D_{calc} [g cm^{-3}]	1.300	1.319	1.316	1.331
T [K]	293	293	293	293
Absorption coefficient [mm^{-1}]	1.393	1.454	1.552	1.597
F(000)	2120	2172	2144	2244
θ range [°]	1.34−27.71	1.08−27.65	1.35−27.52	1.07−25.61
Reflections collected	31137	36293	30993	35189
Independent reflections	22778 (R_{int} = 0.0514)	24333 (R_{int} = 0.0800)	22558 (R_{int} = 0.0261)	18406 (R_{int} = 0.0440)
Goodness-of-fit	0.964 (on F^2)	0.838 (on F^2)	0.951 (on F^2)	0.950 (on F)
Final R indices [$I > n\sigma(I)$][a]	$R1$ = 0.0634 (n = 2.0)	$R1$ = 0.0668 (n = 2.0)	$R1$ = 0.0372 (n = 2.0)	R = 0.049 (n = 1.5)
	$wR2$ = 0.1609	$wR2$ = 0.1479	$wR2$ = 0.0864	R_w = 0.046

[a] $R = R1 = \Sigma\|F_o| - |F_c\|/\Sigma|F_o|$. $R_w = [\Sigma w(|F_o| - |F_c|)^2/\Sigma w(F_o)^2]^{1/2}$. $wR2 = \{\Sigma[w(F_o^2 - F_c^2)^2]/\Sigma[w(F_o^2)^2]\}^{1/2}$.

(KBr): $\nu_{C=N}$ = 1623 cm^{-1}. MS (FAB, +ve): m/z = 1020 [M + H]$^+$ for ^{165}Ho. ESI-HRMS (+ve mode, CH_3OH): m/z = 1020.4086 [M + H]$^+$ ($C_{54}H_{61}HoN_7O_3$ requires 1020.4139). $C_{54}H_{60}HoN_7O_3·CH_2Cl_2·H_2O$ (1122.98): calcd. C 58.82, H 5.75, N 8.73; found C 58.51, H 5.68, N 9.02.

Compound 7: $Er(NO_3)_3·5H_2O$ (0.045 g, 0.101 mmol), Py-CHO (0.077 g, 0.304 mmol) and tren (0.015 g, 0.103 mmol) were used. Yield: 0.088 g, 85%, yellow solid, m.p. > 340 °C (decomp). IR (KBr): $\nu_{C=N}$ = 1620 cm^{-1}. MS (FAB, +ve): m/z = 1021 [M + H]$^+$ for ^{166}Er. ESI-HRMS (+ve mode, CH_3OH): m/z = 1023.4086 [M + H]$^+$ ($C_{54}H_{61}ErN_7O_3$ requires 1023.4174). $C_{54}H_{60}ErN_7O_3·0.75H_2O$ (1035.87): calcd. C 62.60, H 6.00, N 9.47; found C 62.64, H 5.82, N 9.88.

Compound 8: $Tm(NO_3)_3·6H_2O$ (0.047 g, 0.102 mmol), Py-CHO (0.077 g, 0.304 mmol) and tren (0.015 g, 0.103 mmol) were used. Yield: 0.052 g, 50%, greenish-yellow solid, m.p. > 250 °C (decomp). IR (KBr): $\nu_{C=N}$ = 1623 cm^{-1}. MS (FAB, +ve): m/z = 1024 [M + H]$^+$ for ^{169}Tm. ESI-HRMS (+ve mode, CH_3OH): m/z = 1024.4192 [M + H]$^+$ ($C_{54}H_{61}N_7O_3Tm$ requires 1024.4178). $C_{54}H_{60}N_7O_3Tm·1.25H_2O$ (1046.55): calcd. C 61.96, H 6.03, N 9.37; found C 61.97, H 6.00, N 9.37.

Compound 9: $Lu(NO_3)_3·H_2O$ (0.036 g, 0.100 mmol), Py-CHO (0.077 g, 0.304 mmol) and tren (0.015 g, 0.103 mmol) were used. Yield: 0.066 g, 63%, yellow solid, m.p. > 220 °C (decomp). ^{1}H NMR (CD_3OD): δ = 1.35 (s, 27 H, *t*Bu), 2.81 and 3.10 (2 × t, $J_{H,H}$ = 6.5 Hz, 2 × 6 H, 3 × NCH_2CH_2N), 7.02 (t, $J_{H,H}$ = 6.5 Hz, 3 H, py-H), 7.15 (m, 3 H, py-H), 7.53 (m, 3 H, py-H), 7.63 (s, 3 H, Ar-H), 8.00 (s, 3 H, Ar-H), 8.11 (d, $J_{H,H}$ = 8.1 Hz, 3 H, py-H), 8.47 (s, 3 H, N=C*H*) ppm. IR (KBr): $\nu_{C=N}$ = 1623 cm^{-1}. ESI-HRMS (+ve mode, CH_3OH): m/z = 1030.4186 [M + H]$^+$ ($C_{54}H_{61}LuN_7O_3$ requires 1030.4243). $C_{54}H_{60}LuN_7O_3·H_2O$ (1048.08): calcd. C 61.87, H 5.97, N 9.36; found C 61.83, H 6.01, N 9.34.

X-ray Crystallography: Pertinent crystallographic data and other experimental details are summarized in Table 5. Crystals of **4**·H_2O, **5**·CH_3OH·0.75H_2O, **6**·1.5H_2O and **7**·2CH_3OH suitable for X-ray diffraction studies were grown by slow evaporation of a solution of the respective compound in methanol. The selected crystal of each complex was mounted on the top of a glass fiber for data collection. Intensity data were collected at 293 K on a Bruker Axs SMART 1000 CCD area-detector diffractometer (for **4**, **5** and **6**) and a Mar Research image plate scanner (for **7**) using graphite-monochromated Mo-K_α radiation (λ = 0.71073 Å). For **4** and **5**, the collected frames were processed with the software SAINT[30] and an absorption correction was applied (SADABS)[31] to the collected reflections. A self-consistent semi-empirical absorption correction based on Fourier coefficient fitting of symmetry-equivalent reflections was applied using the ABSCOR program for **6**. For **7**, interframe scaling was employed for the absorption correction. The space groups of each crystal were determined from the systematic absences and Laue symmetry checks and confirmed by successful refinement of the structures. The structures of all compounds were solved by direct method (SHELXTL^{TM})[32] and refined by full-matrix least-squares analysis. All non-hydrogen atoms were refined anisotropically. Hydrogen atoms were generated in their idealized positions and allowed to ride on their respective parent carbon atoms. CCDC-157465 (**4**), -190555 (**5**), -190556 (**6**) and -212141 (**7**) contain the supplementary crystallographic data for this paper. These data can be obtained free of charge at www.ccdc.cam.ac.uk/conts/retrieving.html [or from the Cambridge Crystallographic Data Centre, 12, Union Road, Cambridge CB2 1EZ, UK; fax: (internat.) +44-1223/336-033; E-mail: deposit@ccdc.cam.ac.uk].

Acknowledgments

Thanks are due to the Hong Kong Baptist University and the Hong Kong Research Grants Council (HKBU 2038/02P) for financial support.

 © 2004 Wiley-VCH Verlag GmbH & Co. KGaA, Weinheim

[1] A. Smith, S. J. Rettig, C. Orvig, *Inorg. Chem.* **1988**, *27*, 3929−3934.
[2] D. J. Berg, S. J. Rettig, C. Orvig, *J. Am. Chem. Soc.* **1991**, *113*, 2528−2532.
[3] S. Liu, L. Gelmini, S. J. Rettig, R. C. Thompson, C. Orvig, *J. Am. Chem. Soc.* **1992**, *114*, 6081−6087.
[4] S. Liu, L.-W. Yang, S. J. Rettig, C. Orvig, *Inorg. Chem.* **1993**, *32*, 2773−2778.
[5] P. Guerriero, S. Tamburini, P. A. Vigato, *Coord. Chem. Rev.* **1995**, *139*, 17−243.
[6] J.-C. G. Bünzli, C. Piguet, *Chem. Rev.* **2002**, *102*, 1897−1928.
[7] R. Rodríguez-Cortiñas, F. Avecilla, C. Platas-Iglesias, D. Imbert, J.-C. G. Bünzli, A. de Blas, T. Rodríguez-Blas, *Inorg. Chem.* **2002**, *41*, 5336−5349.
[8] P. Caravan, J. J. Ellison, T. J. McMurry, R. B. Lauffer, *Chem. Rev.* **1999**, *99*, 2293−2352.
[9] M. Kanesato, T. Yokoyama, O. Itabashi, T. M. Suzuki, M. Shiro, *Bull. Chem. Soc. Jpn.* **1996**, *69*, 1297−1302.
[10] M. Kanesato, T. Yokoyama, T. M. Suzuki, *Chem. Lett.* **1997**, 93−94.
[11] M. W. Essig, D. W. Keogh, B. L. Scott, J. G. Watkin, *Polyhedron* **2001**, *20*, 373−377.
[12] P. V. Bernhardt, B. M. Flanagan, M. J. Riley, *Aust. J. Chem.* **2001**, *54*, 229−232.
[13] P. Bhattacharyya, J. Parr, A. T. Ross, A. M. Z. Slawin, *J. Chem. Soc., Dalton Trans.* **1998**, 3149−3150.
[14] J.-P. Costes, F. Dahan, A. Dupuis, S. Lagrave, J.-P. Laurent, *Inorg. Chem.* **1998**, *37*, 153−155.
[15] J.-P. Costes, F. Dahan, A. Dupuis, J.-P. Laurent, *Chem. Eur. J.* **1998**, *4*, 1616−1620.
[16] J.-P. Costes, F. Dahan, A. Dupuis, *Inorg. Chem.* **2000**, *39*, 165−168.
[17] J.-P. Costes, F. Nicodème, *Chem. Eur. J.* **2002**, *8*, 3442−3447.
[18] W.-K. Wong, H. Liang, W.-Y. Wong, Z. Cai, K.-F. Li, K.-W. Cheah, *New J. Chem.* **2002**, *26*, 275−278.
[19] S. I. Klink, L. Grave, D. N. Reinhoudt, F. C. J. M. van Veggel, M. H. V. Werts, F. A. J. Geurts, J. W. Hofstraat, *J. Phys. Chem. A* **2000**, *104*, 5457−5468.
[20] Z. R. Reeves, K. L. V. Mann, J. C. Jeffery, J. A. McCleverty, M. D. Ward, F. Barigelletti, N. Armaroli, *J. Chem. Soc., Dalton Trans.* **1999**, 349−355.
[21] Y. Kawamura, Y. Wada, S. Yanagida, *Jpn. J. Appl. Phys.* **2001**, *40*, 350−356.
[22] G. F. de Sá, O. L. Malta, C. de Mello Donegá, A. M. Simas, R. L. Longo, P. A. Santa-Cruz, E. F. da Silva Jr., *Coord. Chem. Rev.* **2000**, *196*, 165−195.
[23] R. Reisfeld, C. K. Jorgensen. *Lasers and Excited States of Rare Earths*, Springer, Berlin, **1977**.
[24] W. T. Carnall, G. L. Goodman, K. Rajnak, R. S. Rana, *J. Chem. Phys.* **1989**, *90*, 3443−3457.
[25] M. Latva, H. Takalo, V. M. Mukkala, C. Matachescu, J.-C. Rodriguez-Ubis, J. Kankare, *J. Luminesc.* **1997**, *75*, 149−169.
[26] N. Sabbatini, M. Guardigli, J.-M. Lehn, *Coord. Chem. Rev.* **1993**, *123*, 201−228.
[27] F. Lam, J. X. Xu, K. S. Chan, *J. Org. Chem.* **1996**, *61*, 8414−8418.
[28] C. A. Parker, W. T. Rees, *Analyst (London)* **1960**, *85*, 587−600.
[29] S. R. Meech, D. C. Phillips, *J. Photochem.* **1983**, *23*, 193−217.
[30] *SAINT, Reference Manual*, Siemens Energy and Automation, Madison, WI, **1994−1996**.
[31] G. M. Sheldrick, SADABS, Empirical Absorption Correction Program, University of Göttingen, **1997**.
[32] G. M. Sheldrick, *SHELXTL*™, *Reference Manual*, v*er.5.1*, Siemens, Madison, WI, **1997**.

Received June 9, 2003
Early View Article
Published Online January 19, 2004

 © 2004 Wiley-VCH Verlag GmbH & Co. KGaA, Weinheim